World Academy of Science, Engineering and Technology
International Journal of Aerospace and Mechanical Engineering
Vol:6, No:8, 2012

CFD Simulations of Flow in Capillary Flow Liquid Acquisition Device Channel

John B. McQuillen, David F. Chao, Nancy R. Hall, Brian J. Motil, Nengli Zhang

***Abstract*—**Future space vehicles will require the use of non-toxic, cryogenic propellants, because of the performance advantages over the toxic hypergolic propellants and also because of the environmental and handling concerns. A prototypical capillary flow liquid acquisition device (LAD) for cryogenic propellants was fabricated with a mesh screen, covering a rectangular flow channel with a cylindrical outlet tube, and was tested with liquid oxygen (LOX). In order to better understand the performance in various gravity environments and orientations with different submersion depths of the LAD, a series of computational fluid dynamics (CFD) simulations of LOX flow through the LAD screen channel, including horizontally and vertically submersions of the LAD channel assembly at normal gravity environment was conducted. Gravity effects on the flow field in LAD channel are inspected and analyzed through comparing the simulations.

***Keywords*—**Liquid acquisition device, cryogenic propellants, CFD simulation, vertically submerged screen channel, gravity effects.

I. Introduction

AS is well known, for a space mission liquid propellants have to be delivered from their storage tanks to an engine in liquid state. It is easy to realize the delivery on earth using gravity to position liquid above the tank outlet that is located at the tank bottom, as shown in Fig. 1a. However, it is impossible to ensure the propellants drainage from the tank without vapor or pressurized gas entrainment in the low gravity environment of space because of the uncertainty of the ullage position. For example, the ullage may cover the outlet some times, as shown in Fig. 1b. A conceptual design of four screen-channel LADs installed inside a propellant tank was presented, as shown in Fig. 1c [1]. The open area of the screen channels is covered with a tight mesh screen. Liquid in the tank passes through the mesh screen and then flows in the screen-channels towards the outlet. It should be noted that in the vapor area no vapor passes through the screen because the liquid wetted the mesh screen prohibits vapor from entering into the channel, as shown in Fig.1d. The performance of capillary flow propellant acquisition/expulsion devices has been a critical research and development concern for space missions. Many of these devices have been built, tested and used for hypergolic propellants, such as nitrogen tetroxide (N_2O_4) and monomethyl hydrazine (MMH), but the development for use with cryogenic propellants has been lagging.

J. B. McQuillen is with NASA Glenn Research Center, Cleveland, OH 44135 USA (e-mail: john.b.mcquillen@nasa.gov).

D. F. Chao is with NASA Glenn Research Center, Cleveland, OH 44135 USA (e-mail: david.f.chao@nasa.gov).

N. R. Hall is with NASA Glenn Research Center, Cleveland, OH 44135 USA (e-mail: nancy.r.hall@nasa.gov).

B. J. Motil is with NASA Glenn Research Center, Cleveland, OH 44135 USA (e-mail: brian.j.motil@nasa.gov).

Nengli Zhang is with Ohio Aerospace Institute at NASA Glenn Research Center, Cleveland, OH 44135 USA (corresponding author to provide phone: 216-433-8750; fax: 216-433-8050; e-mail: nengli.zhang@grc.nasa.gov).

LADs are custom designed to fulfill a unique set of requirements under the appropriate environmental conditions for a particular mission; consequently, there is no universal design that satisfies all applications [2]. Future space vehicles will require the use of non-toxic, cryogenic propellants, because of the performance advantages over the toxic hypergolic propellants and also because of the environmental and handling concerns [3]. Due to conflicting vehicle requirements, the "settling" method previously used to position cryogenic propellants over the tank outlet will have to be relinquished for some future missions necessitating the need for a capillary flow LAD [4]. Capillary flow LADs have been well characterized for storable toxic propellants [3, 5], but there have been only a few LAD experiments with cryogenic propellants, including liquid oxygen (LOX). Because the available measurement technologies are limited when using cryogenic liquids, detailed pressure and velocity distributions in the LAD channel have not been revealed. Computational fluid dynamics (CFD)simulations can provide this information, thus leading to insight into the flow with LAD screen channel and potentially increased performance.

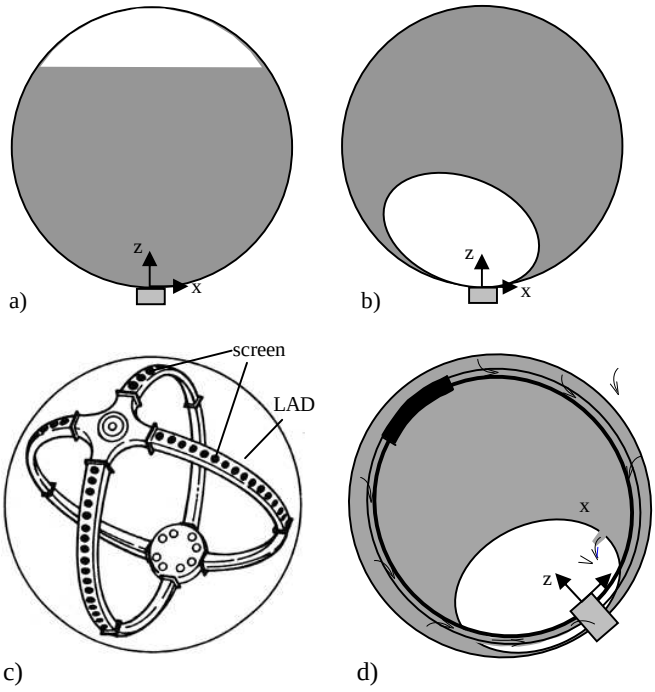

Fig. 1 Liquid propellant delivery on earth and microgravity environments

Recently, Zhang et al [6] performed a CFD simulation for sub-cooled LOX flow in LAD channel test assembly in normal gravity environment. McQuillen et al [7] conducted a series of CFD simulations of the LOX flows in the LAD channel in different gravity environments, including on earth (9.81 m/s^2),

on moon (1.6667 m/s^2), and in space (0.0 m/s^2), for various flow rates. All of these simulations are for the horizontally submerged LAD channel in the LOX. Another important issue for the performance of the screen channel is the orientation and submerged depth effects of the LAD channel in normal gravity environment on the pressure and flow fields in the channel, and the mass flow rate passing through the channel. It is one of important concerns for liftoff period and first-stage of missions. This paper reports the simulation results for various vertically-submerged depths of the LAD channel assembly in the LOX at normal gravity environment. The gravity effects on the flow in the screen channel have been revealed.

II. LAD Channel Test Assembly And Porous Jump Model For Screen

Under NASA's continuing Cryogenic Fluid Management (CFM) development program, a prototypical LAD screen channel assembly was designed and tested using LOX. The LAD channel geometry has been reported in previous papers [6, 7], whose channel geometry is as follows: The flow channel is 609.6 mm (24 in) long by 50.8 mm (2 in) wide by 25.4 mm (1 in) deep. A lip along the top of the channel framed a screen window of 482.6 mm (19 in) long by 50.8 mm (2 in) wide and facilitated the attachment of the screen section to the channel. The outlet-tube has an inner diameter of 23.622 mm (0.93 in). The LOX flows into the channel assembly via the gap between the cover plate and the mesh screen, so called entrance gap, from all directions, and then passes through the fine mesh screen to flow down of the channel assembly and then goes out, as shown in Fig. 2. Since most liquids, including LOX, perfectly wet on stainless steel surfaces, capillary forces drive the liquid to wet the entire screen when the porous screen partially contacts the liquid pool, thus effectively blocking gas passage through the porous screen unless a critical pressure differential, so-called bubble point, is exceeded. The procedure for the bubble-point test is described in American Society for Testing and Materials Standard (ASTM) Method F316. The theoretical relation between the effective pore diameter D_p and the bubble-point pressure Δp_{bp} is:

$$D_p = 4\sigma\cos\theta/\Delta p_{bp} \quad (1)$$

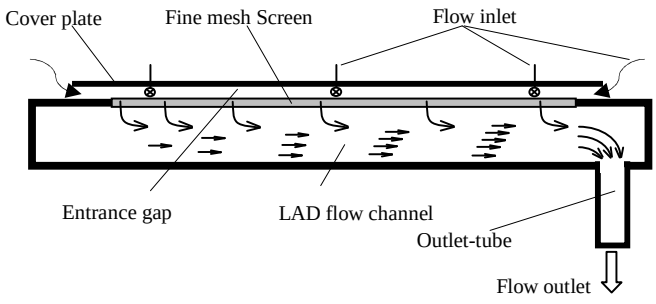

Fig. 2 Fluid flow route in the LAD channel assembly

where σ is the surface tension of the liquid, and θ is the contact angle of the liquid on the screen material. According to the measurement results by Kudlac and Jurns [3], the bubble point for the screen weave of 200x1400 Dutch Twill mesh in LOX is 9.5 inch H_2O (2366 Pa) while the surface tension of LOX is 0.0132 N/m at normal boiling point conditions.

In order to determine flow resistance across the mesh screen, Armour and Cannon [8] developed a general correlation applicable to the flow through all types of woven metal screens, which is

$$f = a/Re + b \quad (2)$$

where $f = \Delta p\varepsilon^2 D/(Q\delta\rho V^2)$, $Re = \rho V/(\mu s^2 D)$, a = 8.61 *and* b = 0.52, in which Δp is the pressure drop when fluid flow passing through the screen, while the parameters Q, ε, D, δ, and s are the tortuosity factor, the void fraction, the pore diameter, the screen thickness, and the surface area to unit volume ratio, respectively, which have been determined by Armour and Canon through their analysis and measurements for each specified screen; ρ, μ, and V are the density, viscosity, and approaching velocity of the fluid passing through the screen. In fact, Eq. (2) can be directly written as

$$\Delta p = AV + BV^2 \quad (3)$$

where $A = 8.61Q\delta\mu s^2/\varepsilon^2$; $B = 0.52Q\delta\rho/\varepsilon^2 D$.

Cady [9] found that the constants $a = 8.61$ and $b = 0.52$ in Eq. (2) are only applicable well to the screen of Plain Dutch mesh 24x110, while considerable errors occur in other screens. He revised Eq. (2) with different values of a and b for each specified screen. For the screen of Dutch Twill mesh 200x1400, he gives $a = 4.2$ and $b = 0.20$, while Q = 1.3, ε = 0.248, D = 0.000010 m, δ = 0.0001524 m, s = 65390 1/m.

It is noted that the relevant parameters determined by Armour and Cannon are based on the experimental data of liquid nitrogen while by Cady based on the experimental data of liquid hydrogen and other data available in literature, including Armour and Cannon's data.

Recently, the research group of CFM development program has measured the pressure drops of LOX flow passing through the screen at various approaching velocities passing through the screen and then directly obtained the parameter A = 4.05x10^4 [Pa·s/m] and B = 1.13x10^5 [Pa·s^2/m^2] in Eq. (3).

Since the Dutch Twill mesh screen is very thin and can be taken as a porous sheet, it is treated as a porous jump in the CFD simulations of the LAD channel flow using FLUENT. The flow across the screen is considered as one–dimensional; therefore, the pressure gradient in the screen can be written as

$$dp/dy = D_y\mu V + 0.5\rho C_y V^2 \quad (4)$$

where D_y is the viscous resistance coefficient, and C_y is the inertial resistance coefficient. The pressure gradient is assumed constant across the thickness; consequently, the pressure drop for flow through the screen is

$$\Delta p_{sc} = (D_y\mu V + 0.5\rho C_y V^2)\delta \quad (5)$$

Two major parameters for the porous-jump in FLUENT, the face permeability, defined as $\alpha = 1/D_y$; and the pressure jump

coefficient defined as $C_2 = C_y$, were determined through relating Eq. (3) to Eq. (5):

$$\alpha = \mu\delta/A = 7.32498\text{x}10^{-13}\ [\text{m}^2] \quad (6)$$

$$C_2 = 2B/\rho\delta = 1.29854\text{x}10^{6}\ [1/\text{m}] \quad (7)$$

It can be seen that they are quite difference from ones derived from the data ether provided by Armour and Cannon or by Cady. For example, from Cady's data we obtained $\alpha = \varepsilon^2/(aQs^2) = 2.634\text{x}10^{-12}$ [m^2] and $C_2 = 2bQ/(\varepsilon^2 D) = 8.45473\text{x}10^{5}$ [1/m], respectively [6]. The occurrence of the difference is probably due to they used inappropriate pore diameters to derive the parameters in Eqs. (2) and (3) [7].

III. CFD Simulation Settings

In order to simulate the cases of vertically partial submersions of the LAD channel in LOX, several geometry models have been established, including completely submerged and partially submerged depths of the mesh screen, such as 1/3, 1/2, and 2/3 screen length submerged. In all of the geometry models, the origin of coordinates was positioned at the center of screen top surface. For partially submerged cases, the exposed portion of the mesh screen was taken as a solid wall, as show in Fig. 3.

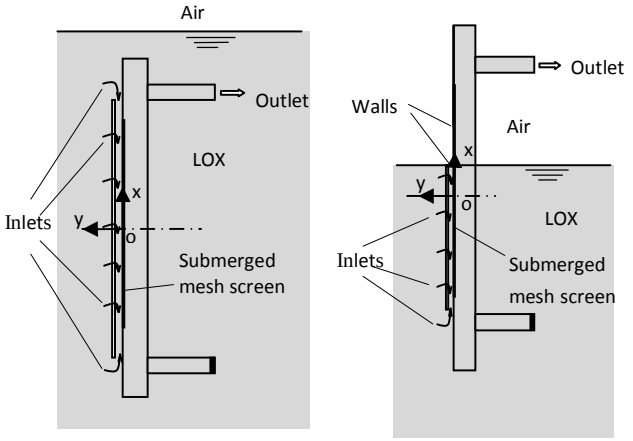

Fig. 3 Vertically submerged LAD channel assembly

This is reasonable because no liquid or vapor can flow through this portion of the screen provided that the local pressure drop between the vapor and the LOX does not exceed the bubble point. The pressure-based solver was used, with a steady implicit formulation. The three-dimensional simulations used the Green-Gauss cell based gradient and the standard k-epsilon model for the turbulent flow with the following constants: the coefficient of first order turbulent dissipation rate in the dissipation rate equation $C_{1\varepsilon} = 1.44$, the coefficient of second order turbulent dissipation rate in the dissipation rate equation $C_{2\varepsilon} = 1.92$, the turbulent viscosity coefficient $C_\mu = 0.09$, the turbulent Prandtl number for turbulent kinetic energy $\sigma_k = 1.0$, and the turbulent Prandtl number for dissipation rate of turbulent kinetic energy $\sigma_\varepsilon = 1.3$.The operating conditions were set to a system pressure = 1620269 Pa, and gravitational acceleration was set at $g_x = g_z = 0.0$ m/s^2, and $g_y = -9.81$ m/s^2 for the horizontally, completely submerged cases, while $g_y = g_z = 0.0$ m/s^2, and $g_x = -9.81$ m/s^2 for vertically, completely and partially submerged cases. The 'pressure-outlet' type was selected as the boundary condition at the flow outlet surface, and set to a gauge pressure of 0 Pa with a backflow modified turbulent viscosity of 0.001 m^2/s. The 'pressure-inlet' type boundary condition was selected at the flow inlet surface with corresponding values of total gauge pressure and modified turbulent viscosity of 0.001 m^2/s to obtain a mass flow rate within the range of 0.0455 kg/s (0.1 lb/s) ~ 0.1818 kg/s (0.4 lb/s). It should be noted that all the gauge pressures are relative to the operating pressure.

IV. Simulation Results

Twenty four cases of vertically-oriented submerged LAD channel, including six completely submerged, seven 2/3 submerged screen length, five 1/2 submerged screen length, and six 1/3 submerged screen length cases, were simulated. Two cases of horizontally-oriented completely submerged LAD channel were simulated for comparison with the corresponding vertically-oriented completely submerged cases.

A. Effects of Gravity on the Flow in the LAD Channel

The simulation results show that for the completely submerged cases the mass flow rate passing through the LAD channel is not affected by the orientation of the channel. In fact, the total static pressure drop between the inlets and outlet, $\Delta p_{i\text{-}o}$, and submerged portion of the screen determines the mass flow rate. For example, at the cases of completely submerged channel, the value of $\Delta p_{i\text{-}o}$ is proportional to the mass flow rate and independent of channel orientation. However, in the vertically-oriented submerged cases, as more of the screen becomes exposed, a larger $\Delta p_{i\text{-}o}$ is needed to achieve the same mass flow rate, as shown in Fig. 4.

For the vertically-oriented completely submerged cases, the hydrostatic pressures in both entrance gap and LAD flow channel are the same; therefore, gravity has no effects on the flow in the channel. The static pressure field and flow pattern in the channel have no different between the completely submerged cases horizontally and vertically oriented channels. For example, the static pressure fields and the velocity vectors near the outlet tube for both cases are almost identical, as shown in Fig. 5. For completely submerged channel, the velocity vectors at different sections along the channel are also identical in both horizontally and vertically oriented channels. Figure 6 shows the velocity vectors along the channel length at the sections of axial distance of $x = -0.16$ m, $x = 0$ m, and $x = 0.16$ m for completely submerged channels in the case of $\Delta p_{i\text{-}o} = 400$Pa, in which the left ones are for horizontally orientated channel while the right ones for vertically orientated channel. However, gravity affects the flow pattern in the flow channel when a portion of the screen is exposed vertically. At the same $\Delta p_{i\text{-}o}$, the amount of exposed screen length is proportional to the hydrostatic pressure drop between the entrance gap and the LAD flow channel; consequently, when the screen exposed portion increases, the resistance of the flow passing through the flow channel becomes larger. As a result, the flow in the flow channel end by the outlet tube is different for the cases of various screen exposures.

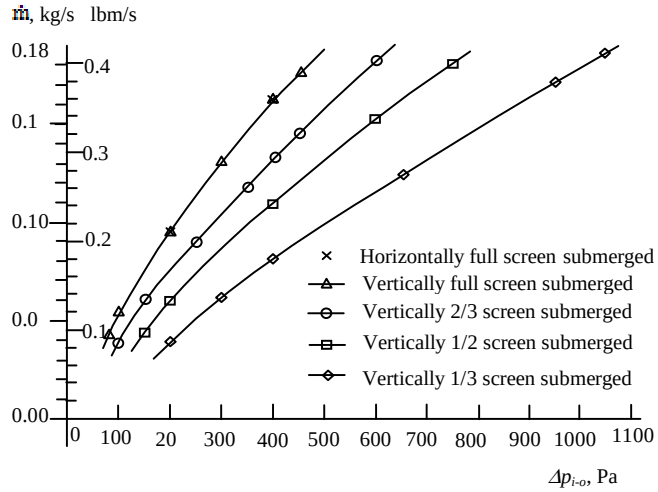

Fig. 4 Mass flow rate vs static pressure drop between the inlet and the outlet

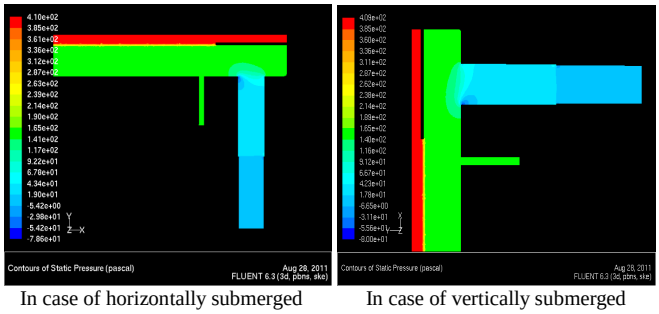

In case of horizontally submerged In case of vertically submerged

a) Pressure field for completely submerged cases

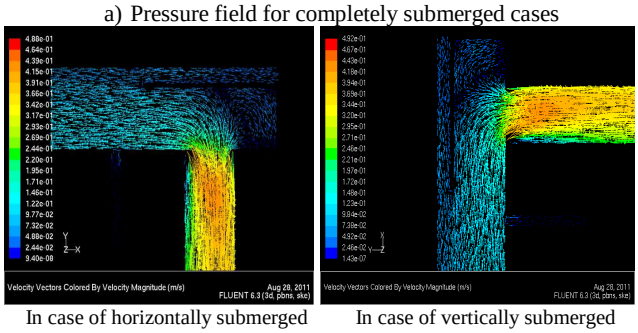

In case of horizontally submerged In case of vertically submerged

b) Velocity vectors for completely submerged cases

Fig. 5 Static pressure fields and velocity vectors in the channel near the outlet tube at $\Delta p_{i\text{-}o}$ = 400 Pa

For the case of vertically-oriented completely submerged channel, the flow has higher velocity in the channel and a vortex occurs at the flow channel end by the outlet tube, as shown in Fig. 5b, while for the cases of vertically-oriented submerged screen half length, the flow enters into the outlet tube without generating vortex, as shown in Fig. 7a, because the higher hydrostatic pressure drop reduces the flow velocity in the flow channel. It should also be noted that for the cases of completely submerged channel and half submerged screen length, the flow direction passing through the screen is different, almost opposite, at the bottom end of the flow channel, as shown in Fig. 7b.

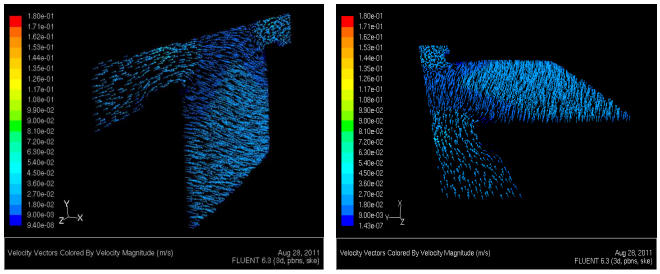

In case of horizontally submerged In case of vertically submerged

a) At section of x = -0.16 m

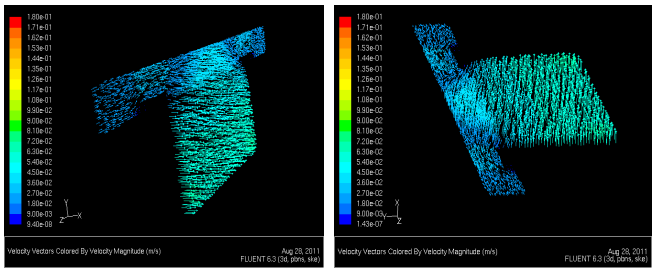

In case of horizontally submerged In case of vertically submerged

b) At section of x = 0 m

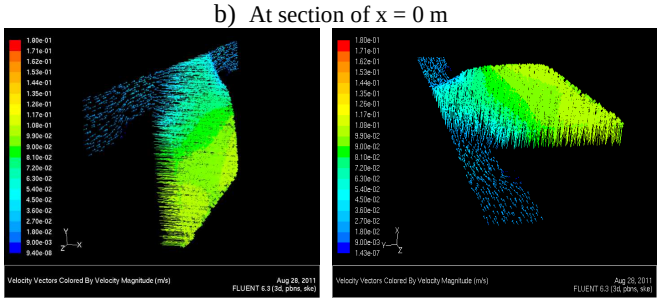

In case of horizontally submerged In case of vertically submerged

c) At section of x = 0.16 m.

Fig. 6 Velocity vectors at different sections for completely submerged cases at $\Delta p_{i\text{-}o}$ = 400 Pa

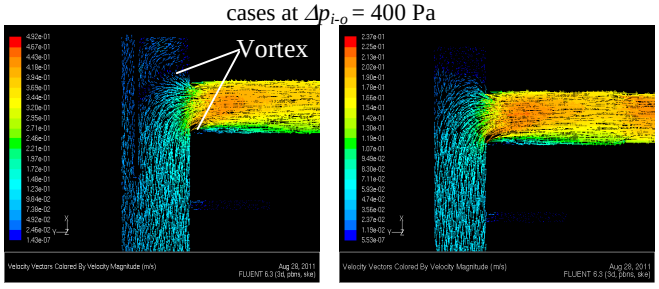

In case of vertically, completely submerged In case of vertically half screen submerged

a) Velocity vectors in the channel near the outlet tube

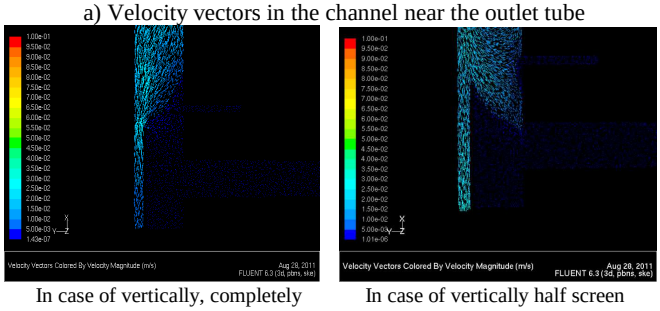

In case of vertically, completely submerged In case of vertically half screen submerged

b) Velocity vectors in the channel at the bottom end of the channel

Fig. 7 Velocity vectors in the channel for the vertically submerged cases at $\Delta p_{i\text{-}o}$ = 400 Pa

B. Mass Flow Rates and Static Pressure in the LAD Channel

The CFD simulation results show that the flow velocity and mass flow rate in the channel are continuously augment along the submerged channel length (x-axis direction) when the LOX passes through the screen and then flows toward the outlet tube in the flow channel. For the vertically partially submerged cases, the mass flow rate in the channel increases along the flow path at the submerged screen portion of the flow channel, and then maintains constant when the LOX flows in the exposed screen portion of the channel because no LOX is added into the channel through the screen anymore. At the same value of $\Delta p_{i\text{-}o}$, although the mass flow rate in the outlet tube in the completely submerged case is much larger than one in the cases of partially submerged screen, the local mass flow rates at any sections in the submerged screen portion of the flow channel for the cases of partially submerged screen are always higher than the corresponding ones of the completely submerged case. For instance, in the cases of vertically oriented 1/3, 1/2, and 2/3 submerged screen length, the submersion terminates at the sections of axial distance of x = -0.08 m, x = 0 m, and x = 0.08 m, respectively, and consequently, the flow rate increases linearly in the channel and reaches maximum at these sections and then maintains constant, as shown in Fig. 8. The typical velocity vectors distributions at different sections for the cases of vertically completely submerged and half submerged screen length are shown in Fig. 9, in which the left ones are for the completely submerged case, while the right ones for the half screen submerged case.

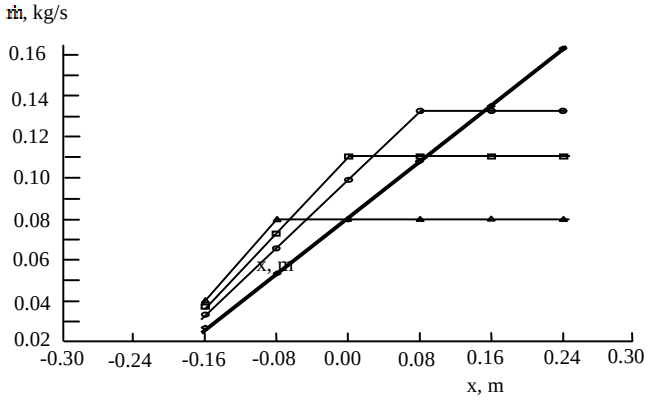

Fig. 8 Mass flow rate, $\dot{m}$, changes along the flow course in the vertically-oriented submerged channels at $\Delta p_{i\text{-}o}$ = 400 Pa

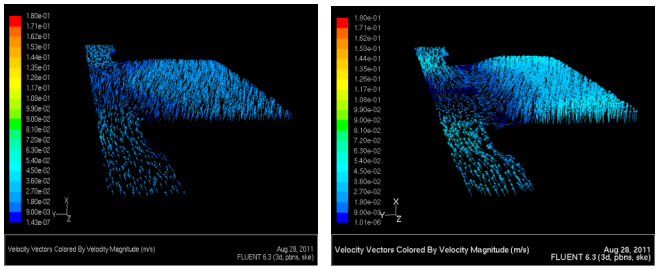

Completely submerged Half screen submerged

a) At section of x = -0.16 m

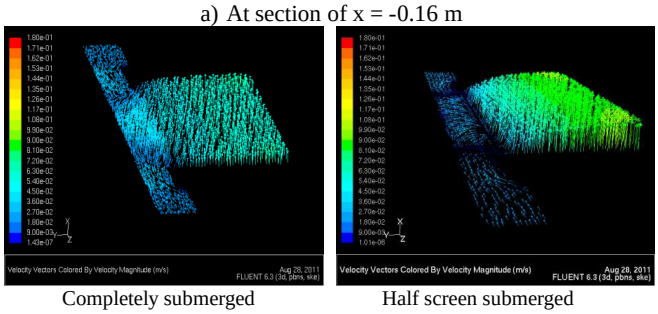

Completely submerged Half screen submerged

b) At section of x = 0 m

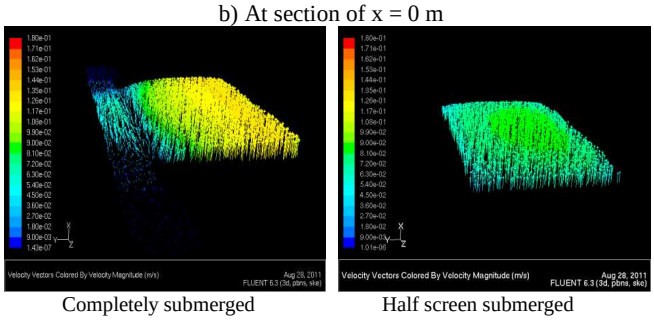

Completely submerged Half screen submerged

c) At section of x = 0.24 m

Fig. 9 Velocity vectors distributions in the vertically oriented submerged channel assembly at $\Delta p_{i\text{-}o}$ = 400 Pa

A typical static pressure distributions along the channel for the cases of vertically submerged LAD assembly at $\Delta p_{i\text{-}o}$ = 400 Pa are shown in Fig. 10. It is seen that in the submerged screen portion of the flow channel, the static pressure decreases nonlinearly, following a parabolic, while in the exposed screen portion of the channel the static pressure linearly decreases. The pressure smoothly transits from the nonlinear decrease to linear decrease along the channel centerline (y = -12.7 mm), but undergoes a small surging near the screen (y = -3 mm) when the LOX flows into the exposed screen portion of the flow channel. It is also noted that for the vertically-oriented submerged cases, at the bottom end of the channel, whose location is far from the outlet tube, the pressure drop between the entrance gap and the LAD flow channel depends on the submerged screen lengths. In the vertically-oriented, completely submerged case at $\Delta p_{i\text{-}o}$ = 400 Pa, the pressure drop between the entrance gap and the flow channel at the bottom end of the channel is about 236 Pa, where the static pressure is 164 Pa, and maintains constant till the screen emerges for no hydrostatic pressure difference between the entrance gap and the LAD flow channel.

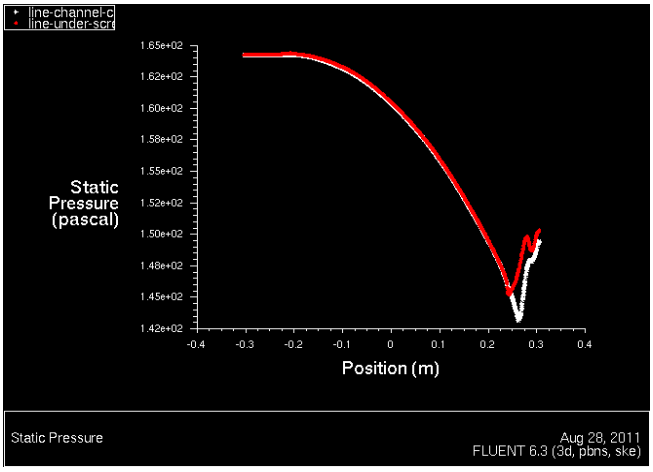

a) In the case of vertically, completely submerged

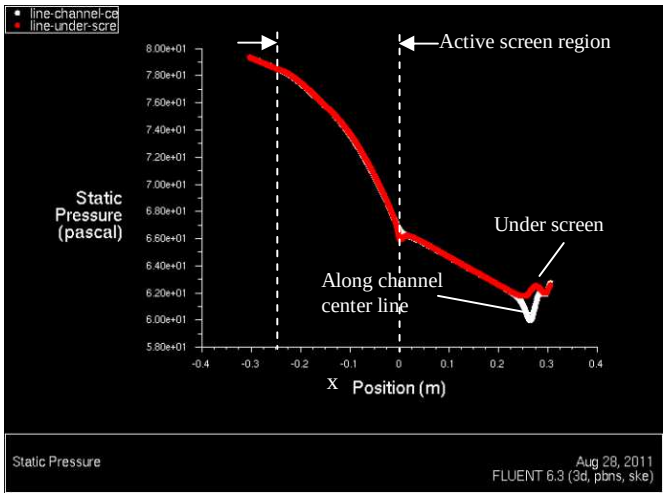

b) In the case of vertically half screen submerged

Fig. 10 Static pressure distributions in the vertically-oriented submerged channel at Δp_{i-o} = 400 Pa

However, in the vertically-oriented partially submerged cases the pressure drop at the bottom end is much higher, for example, in the case of 1/2 submerged screen length, the pressure drop is about 320.5 Pa, where the static pressure is 79.5 Pa only, and linearly increases till the screen emerges because of the effect of gravity, resulting the hydrostatic pressure difference between the entrance gap and the LAD flow channel. After the flow goes out of the active screen region, the pressure drop increases linearly again under the gravity effect. When the flow approaches the outlet tube in the channel, the static pressure undergoes an obvious rebound with a little decrease, as shown in Fig. 10. The static pressure sharply decreases along the centerline of the outlet tube at the entrance section of the tube, as shown in Fig. 11, which is due to the local resistance produced by the sudden change of the flow section area.

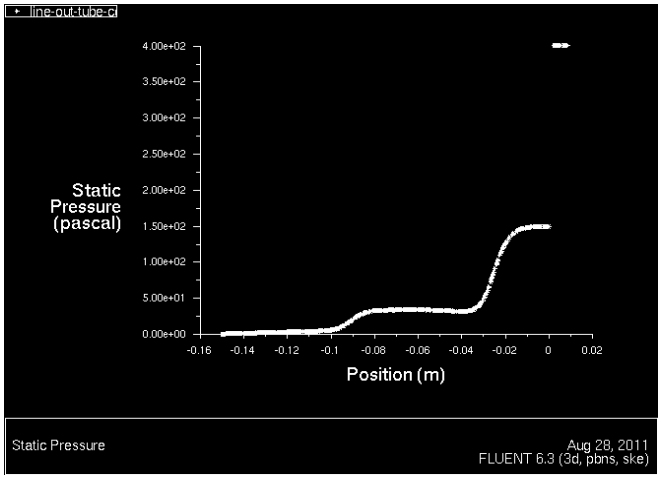

a) In the case of vertically, completely submerged

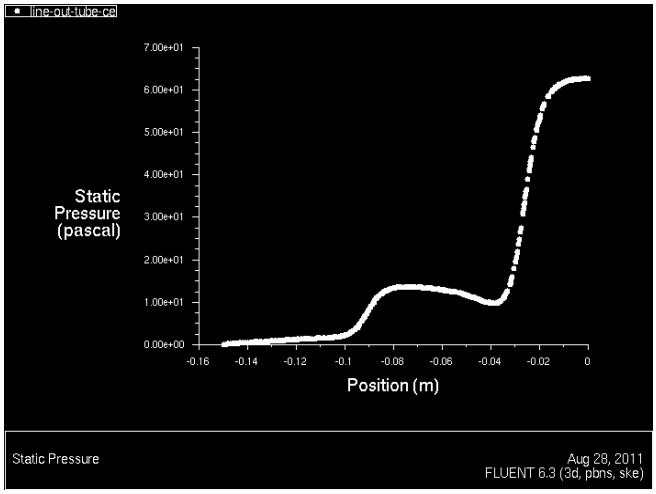

b) In the case of vertically half screen submerged

Fig. 11 Static pressure in the vertically-oriented submerged channel along the outlet tube center line at Δp_{i-o} = 400 Pa

V. Conclusions

1. For the completely submerged cases the mass flow rate passing through the LAD channel are not affected by the orientation of the channel. The mass flow rate is determined by the total static pressure drop between the inlets and outlet, Δp_{i-o}.
2. The gravity affects the flow pattern in the flow channel when different portions of the screen are submerged vertically. At the bottom end of the flow channel, far away from the outlet tube, the hydrostatic pressure drop reverses the flow direction of the LOX passing through the screen, while at the top end of the flow channel the flow smoothly enters into the outlet tube without generating vortex, which is contrary to one in the completely submerged channel cases.
3. For the cases of vertically-oriented partially submerged screen, the mass flow rate increases along the flow course at the submerged portion of the screen in the flow channel, same as the completely submerged cases. However, when the LOX flows in the exposed screen portion of the flow channel, the flow rate maintains constant. The local mass flow rates at any sections in the submerged screen portion of the flow channel

are always higher than the corresponding ones in the completely submerged case.

4. In the vertically submerged screen portion of the flow channel, the static pressure decreases nonlinearly, following a parabolic, while in the exposed screen portion of the flow channel the static pressure linearly decreases under the gravity effect.
5. When the flow approaches the outlet tube in the channel, the static pressure undergoes an obvious rebound with a little decrease. The static pressure sharply decreases along the centerline of the outlet tube at the entrance section of the tube for the local resistance.

REFERENCES

[1] Jurns, j.m. And kudlac, m.t.: liquid acquisition devices evaluated,www.grc.nasa.gov/www/rt/2006/rt/rtp-jurns.html
[2] Fester, d.a., villars, a.j. And uney, p.e.: surface tension propellant acquisition system technology for space shuttle reaction control tanks, j. Spacecraft 13, 522-527 (1976).
[3] Kudlac, m.t. And jurns, j.m.: screen channel liquid acquisition devices for liquid oxygen, 42nd aiaa/asme/sae/asee joint propulsion conference & exhibit, sacramento, ca (2006), see also paper aiaa 2006-5054.
[4] Dyke, m.v.: identification of influential factors for liquid acquisition device designs, 34th joint propulsion conference and exhibit, cleveland, oh (1998), see also paper aiaa-98-3198.
[5] Chato, d.j. And kudlac, m.t.: screen channel liquid acquisition devices for cryogenic propellants, 38th aiaa/asme/sae/asee joint propulsion conference & exhibit, indianapolis, in (2002), see also paper aiaa 2002-3983.
[6] Zhang, n., chato, d.j., mcquillen, j.b., motil, b.j. And chao, d.f.: cfd simulation of pressure drops in liquid acquisition device channel with sub-cooled oxygen, world academy of science, engineering and technology, 58, 1180-1185 (2009).
[7] Mcquillen, j.b., chato, d.j., motil, b.j., doherty, m.p., chao, d.f., and zhang, n.:porous screen applied in liquid acquisition device channel and cfd simulation of flow in the channel, j. Porous media (in print) (2012).
[8] Armour, j.c. And cannon, j.n.: fluid flow through woven screens, j. Aiche, 14, 415-420 (1968).
[9] Cady, e.c.: study of thermodynamic vent and screen baffle integration for orbital storage and transfer of liquid hydrogen, nasa-cr-134482 (1973).
[10] Mcquillen, j.b., chato, d.j., hall, n.r., and zhang, n.: velocity vector field visualization of flow in liquid acquisition device channel, in: proceedings of international conference on information visualization theory and applications, 743-748, rome, italy, 24-26, february, 2012, scitepress digital library.